Research Square

Preprints are preliminary reports that have not undergone peer review.
They should not be considered conclusive, used to inform clinical practice,
or referenced by the media as validated information.

# Casticin sensitizes non-small cell lung carcinoma cells to daunorubicin and mitoxantrone by promoting mitochondrial apoptotic signaling and reducing migratory potential

**Aleksandra Łapa**
Jagiellonian University Medical College, Faculty of Pharmacy
**Natalia Janikowska**
Jagiellonian University Medical College, Faculty of Pharmacy
**Monika Głuch-Lutwin**
Jagiellonian University Medical College, Faculty of Pharmacy
**Barbara Mordyl**
Jagiellonian University Medical College, Faculty of Pharmacy
**Kamil Piska**
Jagiellonian University Medical College, Faculty of Pharmacy
**Aleksandra Pietrzak**
Jagiellonian University Medical College, Faculty of Pharmacy
**Karolina Słoczyńska**
Jagiellonian University Medical College, Faculty of Pharmacy
**Marie Nevyhoštěná**
University of Pardubice, Faculty of Chemical Technology
**Katarzyna Wójcik-Pszczoła**
Jagiellonian University Medical College, Faculty of Pharmacy
**Elżbieta Pękala**
Jagiellonian University Medical College, Faculty of Pharmacy
**Paulina Koczurkiewicz-Adamczyk**
paulina.koczurkiewicz@uj.edu.pl

Jagiellonian University Medical College, Faculty of Pharmacy

**Research Article**

**Keywords:** casticin, non-small cell lung cancer, chemosensitization, cell migration

**Posted Date:** November 27th, 2026

**DOI:** https://doi.org/10.21203/rs.3.rs-11638286/v1

**License:** This work is licensed under a Creative Commons Attribution 4.0 International License.
Read Full License

**Additional Declarations:** No competing interests reported.

# Abstract

Non-small cell lung cancer (NSCLC) remains a major cause of cancer-related mortality owing to intrinsic chemoresistance and early metastatic spread. Strategies that simultaneously enhance chemotherapy efficacy and restrain tumor dissemination are urgently needed. We investigated whether casticin (CAS), a bioactive flavonoid with reported anticancer activity, sensitizes NSCLC cells to daunorubicin (DNR), mitoxantrone (MTX), and cisplatin (CISPL), while defining the molecular basis of its action.

A549 NSCLC cells and non-malignant MRC-5 lung fibroblasts were treated with CAS alone or combined with DNR, MTX, or CISPL. Treatment responses were evaluated by integrated analyses of cell viability, proliferation, mitochondrial function, apoptosis, intracellular $Ca^{2+}$ homeostasis, ERK1/2 signaling, cytoskeletal remodeling, migration, and migration-associated gene expression.

CAS selectively potentiated the antitumor activity of DNR and MTX, but not CISPL, markedly reducing A549 cell viability and proliferation while sparing non-malignant fibroblasts. Chemosensitization was accompanied by robust activation of the mitochondrial apoptotic pathway, evidenced by increased caspase-3/7 activity, cytochrome c release, alterations in mitochondrial morphology, and intracellular $Ca^{2+}$ accumulation, independently of ERK1/2 signaling. Beyond its pro-apoptotic effects, CAS profoundly reorganized actin and vimentin networks, suppressed migratory capacity, and reshaped the expression of migration-associated genes, indicating coordinated inhibition of metastatic traits.

CAS enhanced the activity of two topoisomerase II-targeting agents, suggesting a possible mechanism-dependent interaction that requires direct validation. These findings position CAS as a promising multitarget adjuvant for combination chemotherapy and provide a compelling rationale for its further preclinical and translational development.


# 1. Introduction

Lung cancer remains one of the most frequently diagnosed malignancies and the leading cause of cancer-related mortality worldwide. Approximately 85% of all lung cancer cases are classified as non-small cell lung carcinoma (NSCLC), which constitutes the predominant histological subtype and is frequently characterized by aggressive progression and poor clinical outcome [1]. Despite substantial advances in surgical approaches, targeted therapies, immunotherapy, and platinum-based chemotherapy, the global burden of lung cancer continues to increase, with incidence and mortality rates projected to rise significantly over the coming decades [2–4]. These trends highlights the urgent need for novel therapeutic strategies capable of improving treatment efficacy and overcoming resistance-associated disease progression.

A major obstacle limiting successful NSCLC therapy is the development of chemoresistance, which involves complex molecular adaptations enabling cancer cells to evade cytotoxic stress. These mechanisms include overexpression of multidrug resistance-associated transporters such as P-glycoprotein (P-gp) and multidrug resistance-associated protein 1 (MRP1), dysregulation of

mitochondrial apoptotic signaling, and suppression of pro-apoptotic mediators including BAX and caspase-3, frequently accompanied by increased expression of anti-apoptotic proteins such as BCL-2 [5, 6]. In parallel, the high migratory and metastatic capacity of NSCLC cells is associated with dissemination to the brain, liver, bones, and adrenal glands, contributing to poor prognosis and therapeutic failure, particularly in advanced disease stages [5, 7]. Consequently, contemporary anticancer strategies increasingly focus not only on direct tumor eradication but also on restoring apoptotic susceptibility and limiting metastatic potential.

To address these challenges, considerable attention has been directed toward sensitization-based therapeutic approaches designed to enhance the responsiveness of cancer cells to conventional chemotherapy. Current strategies include combination regimens integrating chemotherapy with photodynamic therapy, immunotherapy, or nanotechnology-based drug delivery systems, all aimed at increasing tumor-selective cytotoxicity and apoptosis induction [8–12]. More recently, naturally derived bioactive compounds have emerged as promising chemosensitizing agents due to their multitarget biological activity, relatively low toxicity, and ability to modulate pathways associated with apoptosis, oxidative stress, and drug resistance.

Among natural compounds investigated in NSCLC models, curcumin and resveratrol have demonstrated the capacity to potentiate the cytotoxic effects of cisplatin through enhanced apoptosis induction and modulation of autophagy-related signaling [13–15]. However, increasing evidence suggests that casticin (CAS), a flavonoid isolated from plants of the *Vitex* genus, may represent a particularly promising candidate for combination-based anticancer therapy [16–18]. Traditionally used in herbal medicine, casticin has recently attracted attention due to its broad spectrum of anticancer activities, including induction of apoptosis, interference with cell cycle progression, suppression of oxidative stress-associated signaling, and inhibition of epithelial–mesenchymal transition (EMT), migration, invasion, and angiogenesis [18–22]. These multifunctional properties suggest that CAS may simultaneously target several hallmarks of cancer progression and therapy resistance.

Despite these promising observations, the chemosensitizing potential of CAS in lung cancer remains poorly understood. Existing evidence is limited primarily to non-solid tumor models or studies focused on attenuation of chemotherapy-associated toxicity rather than enhancement of anticancer efficacy [23, 24]. Consequently, whether CAS can effectively sensitize NSCLC cells to chemotherapy and modulate apoptosis- and migration-associated pathways in solid tumors remains unresolved.

Therefore, the present study aimed to provide the first comprehensive evaluation of casticin as a chemosensitizing agent in NSCLC using the A549 cell model. Particular emphasis was placed on determining whether CAS selectively enhances the anticancer activity of chemotherapeutic agents with distinct mechanisms of action, including cisplatin (CISPL), daunorubicin (DNR), and mitoxantrone (MTX). In addition to evaluating cytotoxic and antiproliferative effects, the study examined mitochondria-mediated apoptotic signaling, intracellular calcium accumulation, ERK1/2 activity, cytoskeletal remodeling, and migration-associated processes to establish a broader mechanistic framework

underlying CAS-mediated sensitization. Importantly, the inclusion of non-malignant MRC-5 lung fibroblasts enabled preliminary assessment of tumor selectivity and potential therapeutic safety. By integrating functional, molecular, and mechanistic analyses, this study provides a novel perspective on the use of natural flavonoids as adjuvant agents capable of restoring chemosensitivity and suppressing aggressive phenotypes in NSCLC cells.

# 2. Material and Methods

### Cell Culture

Human non-small cell lung cancer cells A549 (ATCC CCL-185) and normal human lung fibroblasts MRC-5 (ATCC CCL-171) were employed in this study. The A549 cell line was cultured in F-12K medium (Kaighn's Modification of Ham's F-12 with L-glutamine), whereas MRC-5 fibroblasts were maintained in Eagle's Minimum Essential Medium (EMEM). In both cases, culture media were supplemented with 10% fetal bovine serum (FBS; Gibco, Life Technologies, Waltham, MA, USA) and 1% penicillin–streptomycin solution. Cells were grown under standard incubation conditions (37°C, 5% $CO_2$, 95% humidity). Routine passaging was carried out when cultures reached approximately 80% confluence.

### Experimental model

Mitoxantrone (MTX; *Sigma-Aldrich*; purity ≥ 97%, HPLC), daunorubicin (DNR; *Enzo Life Sciences Inc*.; purity ≥ 90%, assay) and cisplatin (CISPL; *Sigma-Aldrich* purity ≥ 98%, HPLC) were applied separately at concentrations of 0.5, 1, and 2 μM, while casticin (CAS; Sigma-Aldrich; ≥98%, HPLC) was used at 1 μM. Co-treatments with CAS + MTX and CAS + DNR were performed using the same concentrations as in single-compound experiments.

### Cytotoxicity analysis

Cell viability was evaluated using the 3-(4,5-dimethylthiazol-2-yl)-2,5-diphenyltetrazolium bromide (MTT) assay. A549 and MRC-5 cells were seeded in 96-well plates at a density of 5 × $10^3$ cells per well. After 24 h, they were treated with DNR, MTX and CISPL at concentrations of 0.5, 1, and 2 μM, either alone or in co-treatment with CAS 1 μM. Following 24 or 48 h of incubation, MTT reagent (Sigma-Aldrich) was added (final concentration 0.5 mg/ml) to each well and incubated for 3 h (37°C, 5% $CO_2$). The medium was then removed, and the resulting formazan crystals were dissolved in 100 μL of dimethyl sulfoxide (DMSO). Absorbance was measured at 570 nm using a microplate reader (SpectraMax iD3, Molecular Devices, San Jose, CA, USA). All experiments were performed in triplicate using three independent biological replicates. Cell viability was expressed as a percentage of the control according to the formula: viability (%) = (A570sample / A570control) × 100.

### Proliferation Assay

A549 and MRC-5 cells were seeded in 96-well plates at a density of 5 × $10^3$ cells per well. After 24 h, cells were treated with DNR, MTX and CISPL at concentrations of 0.5, 1, and 2 μM, either separately or in co-

treatment with CAS 1 μM. Next, cells were fixed with 3.7% formaldehyde for 15 min, washed with PBS, and stained with 0.01% crystal violet solution for 5 min. The bound dye was eluted using 25% (v/v) methanol solution, containing 1.33% (m/v) citric acid and 1.09% (m/v) sodium citrate. Absorbance was measured at 540 nm using a SpectraMax® iD3 microplate reader (Molecular Devices, San Jose, CA, USA). Cell proliferation was expressed as a percentage of the control according to the formula: proliferation (%) = (A540sample / A540control) × 100. All experiments were performed in triplicate using three independent biological replicates.

**Cytoskeleton organization**

Cells were seeded on sterile glass coverslips placed in 12-well plates, allowed to attach for 24 h, and incubated according to the experimental model. After 24h incubation cells were washed with phosphate-buffered saline (PBS), fixed with 3.7% formaldehyde, permeabilized with 0.1% Triton X-100. Actin filaments were stained with TRITC-conjugated phalloidin and visualized using a fluorescence microscope (Leica Microsystems).

**Immunostaining**

For immunofluorescence analysis, cells were seeded on glass coverslips placed in 12-well plates and cultured for 24 h, followed by incubation with the tested compounds according to the experimental design. After treatment, cells were washed with phosphate-buffered saline (PBS), fixed with 3.7% paraformaldehyde, and permeabilized with 0.1% Triton X-100. Non-specific binding was blocked using 1% bovine serum albumin (BSA). Cells were then incubated overnight at 4°C with primary monoclonal mouse antibodies against vimentin, caspase-3 or cytochrome c (Cell Signaling Technology), followed by incubation with the appropriate Alexa Fluor®–conjugated secondary antibodies. After washing, coverslips were mounted and examined using a fluorescence microscope (Leica Microsystems).

**Caspase-Glo 3/7 Assay**

Apoptotic activity was assessed by quantifying caspase-3/7 activation using the Caspase-Glo® 3/7 Assay (Promega). A549 cells were seeded in 96-well plates at a density of $1 \times 10^4$/well. Cells were incubated with MTX and DNR at concentration of 0.5, 1 μM, CAS, 1 μM, or in co-treatments MTX + CAS or DNR + CAS. After 24h incubation 100 μL of Caspase-Glo® 3/7 reagent was added to each well, and plates were incubated for 1 h at room temperature in the dark, in accordance with the manufacturer's protocol. Luminescence was recorded using a SpectraMax® iD3 microplate reader (Molecular Devices, San Jose, CA, USA).

**Mitochondrial morphology analysis**

For mitochondrial morphology assessment, cells were seeded on sterile glass coverslips placed in 12-well plates at a density of $2 \times 10^4$ cells per well and allowed to attach for 24 h under standard culture conditions. Cells were then incubated with the tested compounds for an additional 24 h. Following treatment, cells were stained with MitoTracker™ Red prepared in FluoroBrite™ medium and incubated for

10 min at 37°C in the dark. After staining, cells were washed with phosphate-buffered saline (PBS), fresh FluoroBrite™ medium was added, and mitochondrial morphology was visualized using a fluorescence microscope (Leica Microsystems).

**High-Content Imaging of the tested compounds**

The A549 cells as described above, were evaluated using High-Content Screening (HCS) fluorescence imaging. After incubation with the compounds, the culture medium was replaced with FluoroBrite DMEM (Thermo Fisher) supplemented with 5 µM Fluo-4 AM. Fluo-4 AM fluorescence was used to assess intracellular $Ca^{2+}$ levels. Following a 1h incubation at 37°C, fluorescence images were performed using the ImageXpress Micro XLS High-Content Screening System (Molecular Devices, USA) and analyzed using MetaXpress software.

**ERK1/2 Phosphorylation Assay**

A549 cells were used to assess compound-induced ERK1/2 phosphorylation using the AlphaLISA SureFire ERK1/2 Phosphorylation assay kit, following the manufacturer's instructions (PerkinElmer). Cells were seeded at $3\times 10^4$ cells per well in a 96-well plate and incubated night at 37°C in a humidified 5% $CO_2$ atmosphere. Test compounds were prepared by serial dilution and added to the cells for 24 hours incubation. The medium was then removed and replaced with lysis buffer. After overnight freezing, 10 µL of each lysate was transferred to assay plates, the AlphaLISA SureFire Ultra reaction mix (PerkinElmer) was added, and plates were incubated according to the kit protocol. Fluorescence signals were recorded using an EnVision plate reader (PerkinElmer Life Sciences).

**Transwell®**

Cancer cell migration was assessed using Transwell® chambers. Prior to cell seeding, both chambers were pre-incubated with serum and antibiotic-free medium for 1 h under standard culture conditions. The medium in the lower chamber was then replaced with medium containing 1% FBS as a chemoattractant. A549 cells were seeded into the upper chamber at a density of $2.5 \times 10^4$ cells/chamber in serum-free medium. After cell attachment, the tested compounds were added to the upper chamber according to the experimental design. Following 24 h of incubation, non-migrated cells on the upper surface of the membrane were removed by cotton swab, while migrated cells on the lower surface were fixed with 3.7% formaldehyde and stained with crystal violet. Migrated cells were visualized and analyzed using a Leica DMI1 light microscope.

**Wound healing assay**

Cell migration was evaluated using a wound healing assay. A549 cells were seeded in 12-well plates at a density of $3 \times 10^5$ cells per well and cultured until a confluent monolayer was formed. Linear wounds were generated manually using a sterile pipette tip. Detached cells were subsequently removed by gentle washing, and fresh culture medium containing the tested compounds was then added. Wound closure was monitored after 24 and 48 h using an inverted light microscope (Leica Microsystems).The wound

area was quantified using ImageJ software (Fiji distribution) and expressed as a percentage of the initial wound area.

**Quantitative real-time PCR (RT–qPCR) analysis**

The expression of selected genes was analyzed by quantitative real-time PCR (RT–qPCR). A549 cells were seeded in 6-well plates at a density of 2.5 × $10^5$ cells per well and cultured for 24 h under standard conditions. Cells were then treated with the tested compounds according to the experimental design. After 24 h, total RNA was isolated using the GeneMATRIX Universal RNA Purification Kit (EURx, Poland), following the manufacturer's instructions. RNA concentration and purity were assessed spectrophotometrically. Complementary DNA (cDNA) was synthesized from 1 µg of total RNA using the iScript™ cDNA Synthesis Kit (Bio-Rad). Quantitative PCR was performed using SsoAdvanced™ Universal SYBR® Green Supermix (Bio-Rad) on a real-time PCR system. Gene-specific primers *CDH1, SNAI, 18S rRNA* (reference) are listed in Table 1. Relative gene expression levels were calculated using the ΔΔCt method and normalized to 18S rRNA. All reactions were performed in triplicate.

Table 1
Gene-specific primers used for real-time PCR analysis

| Gene name | Primer type | Sequence |
|---|---|---|
| **CDH1** | forward | 5' CCTGGGACTCCACCTACAGA 3' |
| | reverse | 5' CCAGAAACGGAGGCCTGATG 3' |
| **SNAI** | forward | 5' CCAGTGCCTCGACCACTATG 3' |
| | reverse | 5' CTGCTGGAAGGTAAACTCTGG 3' |
| **18sRNA** | forward | 5' CGCCGCTAGAGGTGAAATTC 3' |
| | reverse | 5' TTGGCAAATGCTTTCGCTC 3' |

# 3. Results

### 3.1. CAS enhances the cytotoxic effects of DNR and MTX, but not CISPL, in A549 cells while exerting limited effects on MRC-5 fibroblasts

To investigate whether CAS may enhance the anticancer activity of selected chemotherapeutic agents in lung cancer cells, its influence on the cytotoxic effects of daunorubicin (DNR), mitoxantrone (MTX), and cisplatin (CISPL) was evaluated in A549 lung adenocarcinoma cells. In parallel, the effects of the combined treatments were assessed in non-malignant MRC-5 lung fibroblasts to estimate their potential toxicity toward normal cells (Fig. 1).

Cell viability was determined using the MTT assay after 24 h and 48 h of incubation with DNR, MTX, and CISPL at concentrations of 0.5, 1, and 2 µM, administered either alone or in combination with CAS. The results showed that co-treatment with CAS enhanced the cytotoxic effects of DNR and MTX in A549

cells, whereas no additional effect was observed for CISPL. After 24 h of incubation, the combination of DNR and CAS significantly reduced A549 cell viability at 1 and 2 μM compared with DNR alone. Following 48 h exposure, this effect became more pronounced, as a statistically significant reduction in viability was also observed at 0.5 and 1 μM DNR. A similar trend was observed for MTX. After 24 h, the MTX + CAS combination significantly decreased cell viability at 0.5 and 2 μM compared with MTX alone, whereas after 48 h a significant reduction was detected only at 1 μM. In contrast, the combination of CAS and CISPL did not significantly affect A549 cell viability at any tested concentration or incubation time, indicating that the enhancing effect of CAS depended on the chemotherapeutic agent used.

Evaluation of the combined treatments in non-malignant MRC-5 fibroblasts demonstrated limited toxicity after 24 h of incubation. Neither DNR + CAS nor MTX + CAS caused statistically significant changes in cell viability compared with the corresponding chemotherapeutic agents administered alone. After 48 h, although modest but statistically significant reductions in viability were observed for DNR + CAS at 1 μM and for MTX + CAS at 0.5 and 1 μM, cell viability remained above 80% in all groups, indicating substantially lower toxicity toward MRC-5 fibroblasts than toward A549 cancer cells. Likewise, no significant changes in MRC-5 viability were detected following treatment with the CISPL + CAS combination at either incubation time.

Overall, these findings indicate that CAS enhanced the cytotoxic activity of DNR and MTX in A549 lung cancer cells while exerting only limited effects on the viability of non-malignant MRC-5 fibroblasts under the experimental conditions used. Since formal drug interaction analyses were not performed, these results demonstrate enhanced biological effects of the combined treatments rather than pharmacologically confirmed synergistic interactions.

## 3.2. CAS potentiates DNR- and MTX-mediated inhibition of A549 cell proliferation, but not the affects CISPL

Since the MTT assay demonstrated that combined treatment with CAS and selected chemotherapeutic agents reduced A549 cell viability more effectively than the corresponding single-agent treatments, we next examined whether this response was accompanied by a reduction in cell proliferative capacity. To this end, the effects of CAS combined with DNR, MTX, or CISPL on cell proliferation were assessed after 24 h of treatment in A549 lung cancer cells and non-malignant MRC-5 fibroblasts. Cell proliferation was expressed as the percentage of proliferating cells relative to untreated controls (Fig. 2).

The proliferation assay largely confirmed the pattern observed in the viability experiments. In A549 cells, combinations of CAS with DNR or MTX reduced cell proliferation to a greater extent than the corresponding chemotherapeutic agents administered alone, whereas no additional effect was detected for CISPL. Co-treatment with DNR and CAS significantly decreased the proportion of proliferating A549 cells at 1 and 2 μM compared with DNR alone. An even more pronounced response was observed for the MTX + CAS combination, which significantly reduced cell proliferation at all tested concentrations (0.5–2

μM) relative to MTX alone. In contrast, the addition of CAS did not significantly alter the antiproliferative activity of CISPL.

The effects of the combined treatments were substantially less pronounced in non-malignant MRC-5 fibroblasts. DNR + CAS significantly reduced the proportion of proliferating cells only at 1 μM, whereas MTX + CAS did not induce statistically significant changes compared with MTX alone. Likewise, no significant differences were observed between CISPL alone and the CISPL + CAS combination.

Taken together, these findings support the viability data by showing that the greater reduction in A549 cell viability produced by the combinations of CAS with DNR or MTX was accompanied by a corresponding decrease in cell proliferative capacity. In contrast, the combined treatments exerted only limited effects on the proliferative activity of non-malignant MRC-5 fibroblasts, suggesting a preferential effect on the malignant cell line under the experimental conditions used.

## 3.3 CAS potentiates chemotherapy-induced remodeling of actin and vimentin cytoskeleton in A549 cells

The actin cytoskeleton plays a pivotal role in the regulation of cell morphology, adhesion, and migration, thereby contributing to the invasive and metastatic potential of cancer cells. Disruption of cytoskeletal organization is frequently associated with impaired migratory capacity and may additionally reflect the activation of apoptosis-related cellular remodeling processes. Therefore, the effects of CAS in combination with chemotherapeutic agents on the organization of actin filaments and vimentin intermediate filaments in A549 cells were evaluated after 24 h of incubation (Fig. 3).

Because the combined treatments reduced both cell viability and proliferative capacity, we next investigated whether these effects were accompanied by alterations in the organization of the actin and vimentin cytoskeletons, two key structural systems involved in the maintenance of cell morphology, adhesion, and migratory behavior. Since cytoskeletal remodeling is also a characteristic feature of apoptotic cells, actin filaments and vimentin intermediate filaments were examined in A549 cells following 24 h of treatment with CAS administered alone or in combination with DNR or MTX (Fig. 3).

Treatment with DNR alone induced evident reorganization of the actin cytoskeleton, characterized by disruption of filamentous actin and increased perinuclear accumulation of actin structures. Similar changes were observed within the vimentin network, which exhibited marked condensation and redistribution toward the perinuclear region. In contrast, MTX alone caused only modest alterations in actin organization while largely preserving the overall cytoskeletal architecture, although changes in vimentin distribution were also detectable.

The addition of CAS to either DNR or MTX resulted in more pronounced alterations in both actin and vimentin organization than those observed following treatment with the respective chemotherapeutic agents alone. The combined treatments were associated with extensive cytoskeletal disorganization, loss of filament integrity, and enhanced perinuclear redistribution of both cytoskeletal components.

Taken together, these observations indicate that the greater reduction in cell viability and proliferative capacity produced by the combined treatments was accompanied by more extensive cytoskeletal remodeling. Although these structural changes are consistent with impaired cellular organization and reduced migratory capacity, they may also reflect apoptosis-associated cytoskeletal reorganization induced by the treatments.

## 3.4 CAS potentiates DNR- and MTX-induced mitochondrial apoptosis independently of ERK1/2 signaling in A549 cells

The pronounced reduction in cell viability and proliferative capacity observed following the combined treatments, together with the accompanying cytoskeletal remodeling, prompted further investigation into the underlying mechanism of cell death. Therefore, several apoptosis-related parameters were examined in A549 cells following 24 h treatment with DNR or MTX administered alone or in combination with CAS. Intracellular calcium levels were quantified by high-content screening (HCS) as an early regulator of apoptosis, caspase-3/7 activity was measured using a luminescence-based assay, and ERK1/2 phosphorylation was analyzed to determine whether activation of the MAPK/ERK pathway contributed to the observed cellular responses (Fig. 4).

Co-treatment with DNR and CAS significantly increased intracellular calcium levels at both tested concentrations (0.5 and 1 μM) compared with DNR alone, whereas the MTX + CAS combination did not significantly alter calcium accumulation relative to MTX treatment alone. These findings indicate that intracellular calcium mobilization may contribute to the response elicited by the DNR + CAS combination but is unlikely to represent a common mechanism underlying the effects of both drug combinations.

Despite these differences, the combination of CAS with either DNR or MTX produced a concentration-dependent increase in caspase-3/7 activity. In both cases, caspase activation was significantly greater than that observed following treatment with the corresponding chemotherapeutic agents alone, indicating enhanced activation of apoptotic pathways. In contrast, ERK1/2 phosphorylation remained unchanged under all experimental conditions, suggesting that the observed apoptotic response occurred without detectable alterations in ERK1/2 phosphorylation at the examined time point.

To further characterize the apoptotic response, activation of caspase-3 together with cytochrome c localization and mitochondrial morphology were evaluated by immunofluorescence. Cells exposed to DNR + CAS or MTX + CAS exhibited stronger active caspase-3 immunoreactivity than cells treated with the corresponding chemotherapeutic agents alone, corroborating the luminescence assay results. In addition, cytochrome c redistribution from mitochondria to the cytoplasm was more pronounced following the combined treatments, supporting the involvement of the intrinsic mitochondrial apoptotic pathway. Combined exposure to CAS and the chemotherapeutic agents also reduced MitoTracker® fluorescence intensity and induced evident alterations in mitochondrial structure and organization. These observations are consistent with mitochondrial dysfunction during apoptosis but do not provide direct evidence of mitochondrial membrane depolarization.

Taken together, these findings indicate that the enhanced cytotoxic effects of CAS in combination with DNR or MTX are accompanied by increased activation of apoptotic pathways, as reflected by elevated caspase activity, cytochrome c redistribution, and mitochondrial alterations. These effects occurred without detectable changes in ERK1/2 phosphorylation under the experimental conditions examined.

### 3.5 CAS enhances the anti-migratory effects of DNR and MTX and modulates EMT-related gene expression in A549 cells

Given that the combined treatments enhanced apoptotic cell death, we next examined whether these effects were accompanied by reduced migratory capacity of A549 cells. Cell migration was therefore assessed using complementary wound healing and Transwell migration assays, allowing evaluation of both collective two-dimensional migration and directional migration through a porous membrane. To further characterize molecular changes associated with the migratory phenotype, the expression of the migration-related genes *CDH1* and *SNAI1*, encoding E-cadherin and Snail, respectively, was also analyzed (Fig. 5).

Both migration assays demonstrated that the addition of CAS enhanced the inhibitory effects of DNR and MTX on A549 cell migration. In the wound healing assay, the combined treatments reduced wound closure more effectively than the corresponding chemotherapeutic agents alone, with the strongest inhibition observed following MTX + CAS treatment (Fig. 5A). A comparable trend was observed in the Transwell assay, where co-treatment with CAS and either DNR or MTX decreased the number of migrating cells relative to single-agent treatment. Again, the MTX + CAS combination produced the greatest reduction in directional cell migration.

To determine whether these functional changes were accompanied by alterations in migration-associated gene expression, *CDH1* and *SNAI1* transcript levels were evaluated after 24 h of treatment. Combined treatment with DNR and CAS significantly reduced *CDH1* expression compared with DNR alone, whereas no significant change in *CDH1* expression was observed following MTX + CAS treatment. In contrast, *SNAI1* expression was significantly decreased following co-treatment with CAS and either DNR or MTX. Thus, the combined treatments modulated the expression of selected migration-associated genes; however, the transcriptional changes did not indicate a uniform shift toward an epithelial phenotype.

Taken together, these findings demonstrate that CAS enhanced the inhibitory effects of DNR and MTX on A549 cell migration. Although reduced migration was accompanied by altered expression of selected EMT-associated genes, the observed transcriptional profile does not support a straightforward interpretation of EMT inhibition and may instead reflect more complex changes associated with the cellular response to the combined treatments.

## 4. Discussion

Lung cancer remains one of the leading causes of cancer-related mortality worldwide, and resistance to conventional chemotherapy continues to represent a major limitation in the treatment of non-small cell lung carcinoma (NSCLC). Increasing evidence suggests that dysregulation of apoptotic signaling and enhanced migratory potential contribute substantially to therapy failure and tumor progression. Consequently, considerable attention has been directed toward combination strategies employing bioactive natural compounds to improve chemosensitivity and overcome drug resistance.

Several natural compounds have already demonstrated promising chemosensitizing activity in lung cancer models. Hou et al. [25] reported that combined treatment with doxorubicin and resveratrol significantly inhibited proliferation of H69 and H69AR lung cancer cells while reducing expression of multidrug resistance-associated proteins, including P-glycoprotein (P-gp) and MRP1. Similarly, Rui Liu [26] demonstrated that apigenin enhanced cisplatin-induced apoptosis in A549 cells through increased p53 expression. These findings support the concept that natural compounds may improve the efficacy of conventional chemotherapy by modulating apoptotic pathways and resistance-associated mechanisms. Among such bioactive molecules, casticin (CAS), a plant-derived flavonoid, has attracted increasing attention due to its documented anticancer properties, including induction of apoptosis, interference with cell cycle progression, and inhibition of cancer cell migration [19]. Moreover, Piska et al. [27] demonstrated that CAS synergistically enhanced the anticancer activity of abiraterone in prostate cancer models through inhibition of AKR1C3, a key enzyme involved in therapeutic resistance, while simultaneously increasing apoptosis induction. Collectively, these observations suggest that CAS may represent a promising adjuvant candidate in combination-based anticancer strategies.

One of the most important observations emerging from the present study is the selective ability of CAS to enhance the effects of the tested compounds in NSCLC cells. In the initial stage of the study, the ability of CAS to potentiate the effects of selected anticancer compounds was evaluated in A549 cells in combination with cisplatin (CISPL), mitoxantrone (MTX), and daunorubicin (DNR). Although all tested chemotherapeutic agents reduced cancer cell viability, a pronounced potentiating effect of CAS was observed predominantly in combination with DNR and MTX, whereas no comparable enhancement was detected for cisplatin. These findings suggest that the ability of CAS to enhance the effects of chemotherapeutic agents is not universal but may instead depend on the molecular mechanism of action of the co-administered agent.

Importantly, both DNR and MTX are mechanistically associated with topoisomerase II–directed cytotoxicity, raising the possibility that CAS preferentially increases the effects of therapies inducing DNA topology disruption and replication-associated stress in NSCLC cells. This interpretation is strongly supported by the study of Fu et al., who demonstrated that casticin induces apoptosis in NSCLC cells through inhibition of topoisomerase IIα activity [28]. The convergence between these findings and our observations suggests that CAS may functionally amplify cellular responses associated with topoisomerase II inhibition, thereby enhancing mitochondrial stress signaling and apoptotic susceptibility in cancer cells.

Mechanistically, topoisomerase II inhibitors promote DNA double-strand breaks and replication stress, which can trigger mitochondrial apoptotic signaling when cellular repair capacity becomes overwhelmed. In this context, the enhanced caspase-3/7 activation, cytochrome c release, mitochondrial depolarization, and intracellular calcium accumulation observed following CAS co-treatment indicate that CAS may lower the apoptotic threshold of NSCLC cells exposed to topoisomerase II–targeting agents. Rather than acting as a nonspecific cytotoxic enhancer, CAS appears to selectively amplify intrinsic apoptotic competence in chemotherapy-treated cancer cells.

In contrast, no synergistic effect was observed for the combination of CAS with cisplatin under the applied experimental conditions. This difference further supports the concept of mechanistic selectivity underlying CAS activity. Nevertheless, despite the absence of direct chemosensitization in A549 cells, previous in vivo studies demonstrated that CAS exerts hepatoprotective and antioxidant effects during cisplatin treatment, including reduction of ALT, AST, and ALP levels, attenuation of oxidative stress, and protection against histopathological liver injury [18]. Therefore, CAS may still provide therapeutic benefit in cisplatin-based chemotherapy by improving treatment tolerability and limiting systemic toxicity.

Importantly, the effects observed in the present study were substantially more pronounced in A549 cancer cells than in MRC-5 fibroblasts, indicating a degree of tumor selectivity. Although slight reductions in viability and proliferation were detected in MRC-5 cells under selected conditions, these effects remained markedly weaker than those observed in malignant cells. This differential response suggests that CAS may increase the effects of topoisomerase II–directed chemotherapy in NSCLC cells without proportionally increasing toxicity toward normal lung cells, which may be advantageous for the development of combination strategies with an improved therapeutic profile.

The concept of enhancing anticancer efficacy through combination approaches that intensify apoptosis while simultaneously suppressing pro-metastatic traits has been increasingly supported in NSCLC models, including A549 cells. For instance, Eslami et al. demonstrated that combined treatment with dendrosomal curcumin and daunorubicin synergistically inhibited proliferation and migration of A549 cells while significantly enhancing apoptosis, indicating that chemosensitization may be achieved by reinforcing intracellular death programs rather than merely increasing baseline cytotoxicity [29]. These findings are highly consistent with our results, in which CAS co-treatment augmented caspase-3/7 activity, promoted cytochrome c release, altered mitochondrial morphology, and reduced migratory capacity. These findings are further supported by previous reports demonstrating that CAS induces apoptosis in NSCLC cells through inhibition of topoisomerase IIα activity [28]. This observation is mechanistically aligned with our findings, as the most pronounced effects of CAS were observed in combination with topoisomerase II inhibitors, namely daunorubicin and mitoxantrone. The ability of CAS to interfere with topoisomerase II–related signaling may therefore contribute to the amplified apoptotic response observed in our co-treatment settings. Furthermore, recent studies indicate that reduced responsiveness of A549 cells to anthracyclines can be overcome through adjuvant agents or nanomaterials that restore drug sensitivity and enhance cell death signaling pathways [30]. Together,

these reports strengthen the rationale for combination strategies designed to resensitize tumor cells to chemotherapy through modulation of intracellular stress and apoptotic machinery.

More broadly, contemporary mechanistic analyses emphasize that resistance and treatment failure in solid tumors are often associated with dysregulation of mitochondrial apoptosis control and adaptive stress responses rather than with a single dominant resistance pathway [31]. Combined treatment approaches that selectively increase mitochondrial vulnerability in cancer cells are therefore considered particularly promising. This framework fits well with our observations: CAS co-treatment significantly amplified caspase activation and mitochondrial apoptotic features in A549 cells. The involvement of mitochondrial signaling is further supported by recent work highlighting the central role of mitochondrial calcium handling and metabolic regulation in apoptosis induction and therapeutic responsiveness [32]. The elevated intracellular calcium levels detected in the DNR + CAS condition in our study may therefore reflect an upstream event contributing to mitochondrial destabilization and activation of the intrinsic apoptotic pathway. Mechanistically, increased apoptotic responses are frequently linked to intrinsic mitochondrial dysfunction and amplification of pro-apoptotic signaling cascades, which tend to exert a more pronounced effect in cancer cells characterized by elevated basal stress and dysregulated survival pathways. The lack of significant ERK1/2 modulation at the examined time point suggests that the observed increase in treatment effects is unlikely to result from generalized suppression of survival signaling. Instead, CAS appears to preferentially target mitochondrial apoptotic competence, thereby selectively amplifying chemotherapy-induced death signaling. This further supports the hypothesis that CAS enhances chemotherapy response by lowering the apoptotic threshold in malignant cells.

Taken together, the present findings support the premise that combined treatment approaches targeting apoptosis and migration, such as CAS co-treatment with topoisomerase II inhibitors, may increase anticancer effects in NSCLC cells while inducing limited additional toxicity in non-malignant cells. The observed suppression of migratory activity together with reduced *SNAI* expression indicates that CAS may partially interfere with EMT-associated signaling pathways, which are critically involved in metastatic dissemination and therapy resistance in NSCLC. The observed tumor-selective enhancement, combined with mitochondrial pathway engagement and suppression of migratory potential, underscores the translational relevance of this approach. Nevertheless, further mechanistic studies and in vivo validation are warranted to confirm the therapeutic potential of CAS as an adjuvant agent in lung cancer treatment.

## Limitations of the Study

Although the present study provides important insight into the effects of CAS in combination with chemotherapeutic agents in NSCLC cells, several limitations should be acknowledged. First, the experiments were performed using a single NSCLC cell line (A549), which represents only one molecular subtype of this heterogeneous disease. Therefore, validation in additional NSCLC models with distinct genetic backgrounds or resistance phenotypes would further strengthen the generalizability of the findings.

Second, the study was conducted exclusively under in vitro conditions. While this approach enables detailed mechanistic evaluation, it does not fully reflect the complexity of the tumor microenvironment, including stromal interactions, immune regulation, and pharmacokinetic factors that may influence therapeutic responses in vivo. Consequently, further studies using animal models are required to verify the therapeutic efficacy and safety profile of CAS-based combination strategies.

Third, although our findings strongly support the involvement of mitochondrial apoptotic mechanisms, the precise upstream molecular targets underlying the effects of CAS in combination with chemotherapeutic agents remain to be clarified. Future studies investigating mitochondrial membrane dynamics, BCL-2 family proteins, or additional survival-related signaling pathways may provide deeper mechanistic insight. Moreover, while multidrug resistance (MDR) was considered within the conceptual framework of this study, direct analysis of drug transporter activity was beyond its scope and warrants further investigation. Despite these limitations, the present findings provide a strong rationale for further exploration of CAS as a potential component of combination treatment strategies in NSCLC therapy.

## Declarations

# Conflict of Interest:

The authors declare that they have no known competing financial interests or personal relationships that could have appeared to influence the work reported in this paper.

# Author Contribution

Ł.A-wrote the main manuscript text, data curation, investigation, figure preparation N.J-investigation, review and editing, M.G-L-investigation, B.M-investigation,K.P-data curation, review and editing, A.P-review and editing, K.S-review and editing, M.N-investigation, data curation, K.W-P-review and editing, E.P-review and editing, resources, P.K-A-conceptalization, wrote the main manuscript text, data curation, review and editing

## References


1. Nicholson AG et al (2022) The 2021 WHO Classification of Lung Tumors: Impact of Advances Since 2015, Mar. 01, *Elsevier Inc.*10.1016/j.jtho.2021.11.003
2. National Cancer Institute (NCI) Non-Small Cell Lung Cancer Treatment (PDQ®)–Health Professional Version. National Cancer Institute. Available at: https://www.cancer.gov/types/lung/hp/non-small-cell-lung-treatment-pdq. Accessed 17 April 2025
3. Alexander M, Kim SY, Cheng H (2020) Update : Management of Non-Small Cell Lung Cancer, Dec. 01, 2020, *Springer*. 10.1007/s00408-020-00407-5

4. International Agency for Research on Cancer. Global Cancer Observatory. Lyon: World Health Organization (2024) [cited 2026 May 3]. Available from: gco.iarc.who.int/en
5. Hendriks LEL et al (2024) Non-small-cell lung cancer. Dec 01. 10.1038/s41572-024-00551-9
6. Khan SU, Fatima K, Aisha S, Malik F Unveiling the mechanisms and challenges of cancer drug resistance. Feb 12 2024 BioMed Cent Ltd. 10.1186/s12964-023-01302-1
7. Li Y, Yan B, He S Advances and challenges in the treatment of lung cancer. Dec 31 2023 Elsevier Masson s r l 10.1016/j.biopha.2023.115891
8. Kan D et al (2025) Synergistic strategies in photodynamic combination therapy for cancer: mechanisms, nanotechnology, and clinical translation. Front Media SA. 10.3389/fonc.2025.1607259
9. Gong S, Li Q, Yu X, Yang S (2024) Efficacy and safety of different immunotherapies combined with chemotherapy as first-line therapy in patients with small cell lung cancer: a network meta-analysis. Front Media SA. 10.3389/fimmu.2024.1362537
10. Gandhi L et al (May 2018) Pembrolizumab plus Chemotherapy in Metastatic Non–Small-Cell Lung Cancer. N Engl J Med 378:2078–2092. 10.1056/nejmoa1801005
11. Kassaee SN, Richard D, Ayoko GA, Islam N (2024) Lipid polymer hybrid nanoparticles against lung cancer and their application as inhalable formulation. Taylor Francis Ltd. 10.1080/17435889.2024.2387530
12. Hsieh CH et al (2021) An innovative NRF2 nano-modulator induces lung cancer ferroptosis and elicits an immunostimulatory tumor microenvironment. Theranostics 11(14):7072–7091. 10.7150/thno.57803
13. Hong Y, Che S, Hui B, Wang X, Zhang X, Ma H (2020) Combination therapy of lung cancer using layer-by-layer cisplatin prodrug and curcumin co-encapsulated nanomedicine. Drug Des Devel Ther 14:2263–2274. 10.2147/DDDT.S241291
14. Wang L, Hu R, Dai A (2022) Curcumin Increased the Sensitivity of Non-Small-Cell Lung Cancer to Cisplatin through the Endoplasmic Reticulum Stress Pathway, *Evidence-based Complementary and Alternative Medicine*, vol. 2022. 10.1155/2022/6886366
15. Moar K (2024) Synergistic anticancer activity of resveratrol with cisplatin and carboplatin in A549 lung adenocarcinoma cells. Int J Clin Exp Pathol 17(11):411–420. 10.62347/rysq1416
16. He G, Cao X, He M, Sheng X, Wu Y, Ai X (2014) Casticin inhibits self-renewal of liver cancer stem cells from the MHCC97 cell line. Oncol Lett 7(6):2023–2028. 10.3892/ol.2014.2772
17. Zhang J, Cui Y, Sun S, Cao J, Fang X (Apr. 2018) Casticin inhibits the epithelial-mesenchymal transition in ovarian carcinoma via the hedgehog signaling pathway. Oncol Lett 15(4):4495–4502. 10.3892/ol.2018.7880
18. Shih YL et al (Sep. 2017) Casticin impairs cell migration and invasion of mouse melanoma B16F10 cells via PI3K/AKT and NF-κB signaling pathways. Environ Toxicol 32(9):2097–2112. 10.1002/tox.22417

19. Ramchandani S, Naz I, Lee JH, Khan MR, Ahn KS An overview of the potential antineoplastic effects of casticin. Mar 02 2020 MDPI AG. 10.3390/molecules25061287
20. Carbone K et al (2023) Casticin as potential anticancer agent: recent advancements in multi-mechanistic approaches. Front Media S A. 10.3389/fmolb.2023.1157558
21. Lee JH, Kim C, Um JY, Sethi G, Ahn KS (Feb. 2019) Casticin-induced inhibition of cell growth and survival are mediated through the dual modulation of Akt/mTOR signaling cascade. Cancers (Basel) 11(2). 10.3390/cancers11020254
22. Lin CC et al (Jul. 2019) Casticin inhibits human prostate cancer DU 145 cell migration and invasion via Ras/Akt/NF-κB signaling pathways. J Food Biochem 43(7). 10.1111/jfbc.12902
23. Cheng ZY et al (2020) Sep., Combinational treatment of 5-fluorouracil and casticin induces apoptosis in mouse leukemia WEHI-3 cells in vitro, *Environ. Toxicol.*, vol. 35, no. 9, pp. 911–921. 10.1002/tox.22927
24. Umar Ijaz M et al (Jan. 2020) Remedial effects of casticin as an antioxidant on cisplatin induced oxidative damage in rat liver. J King Saud Univ Sci 32(1):1100–1105. 10.1016/j.jksus.2019.10.009
25. Hou C, Lu L, Liu Z, Lian Y, Xiao J (2021) Resveratrol reduces drug resistance of SCLC cells by suppressing the inflammatory microenvironment and the STAT3/VEGF pathway, *FEBS Open Bio*, vol. 11, no. 8, pp. 2256–2265, Aug. 10.1002/2211-5463.13230
26. Liu R et al (Feb. 2017) Apigenin enhances the cisplatin cytotoxic effect through p53-modulated apoptosis. Oncol Lett 13(2):1024–1030. 10.3892/ol.2016.5495
27. Piska K et al (Jan. 2025) Casticin inhibits AKR1C3 and enhances abiraterone efficacy in castration-resistant prostate cancer. J Nat Med. 10.1007/s11418-025-01974-8
28. Fu C, Zhang K, Wang M, Qiu F (Jun. 2022) Casticin and chrysosplenol D from Artemisia annua L. induce apoptosis by inhibiting topoisomerase IIα in human non-small-cell lung cancer cells. Phytomedicine 100:154095. 10.1016/j.phymed.2022.154095
29. Eslami SS et al (2023) Combined Treatment of Dendrosomal-Curcumin and Daunorubicin Synergistically Inhibit Cell Proliferation, Migration and Induce Apoptosis in A549 Lung Cancer Cells. Adv Pharm Bull 13(3):539–550. 10.34172/apb.2023.050
30. Jin W, Yang T, Jia J, Jia J, Zhou X (Jan. 2024) Enhanced Sensitivity of A549 Cells to Doxorubicin with WS2 and WSe2 Nanosheets via the Induction of Autophagy. Int J Mol Sci 25(2). 10.3390/ijms25021164
31. Dhiman VK, Kumari M, Singh D Chemoresistance: The hidden barrier in cancer treatment. Mar 01 2026 Chinese Med Association. 10.1016/j.cpt.2025.07.001
32. Du H, Xu T, Yu S, Wu S, Zhang J Mitochondrial metabolism and cancer therapeutic innovation. Dec 01 2025 Springer Nature. 10.1038/s41392-025-02311-x

# Figures

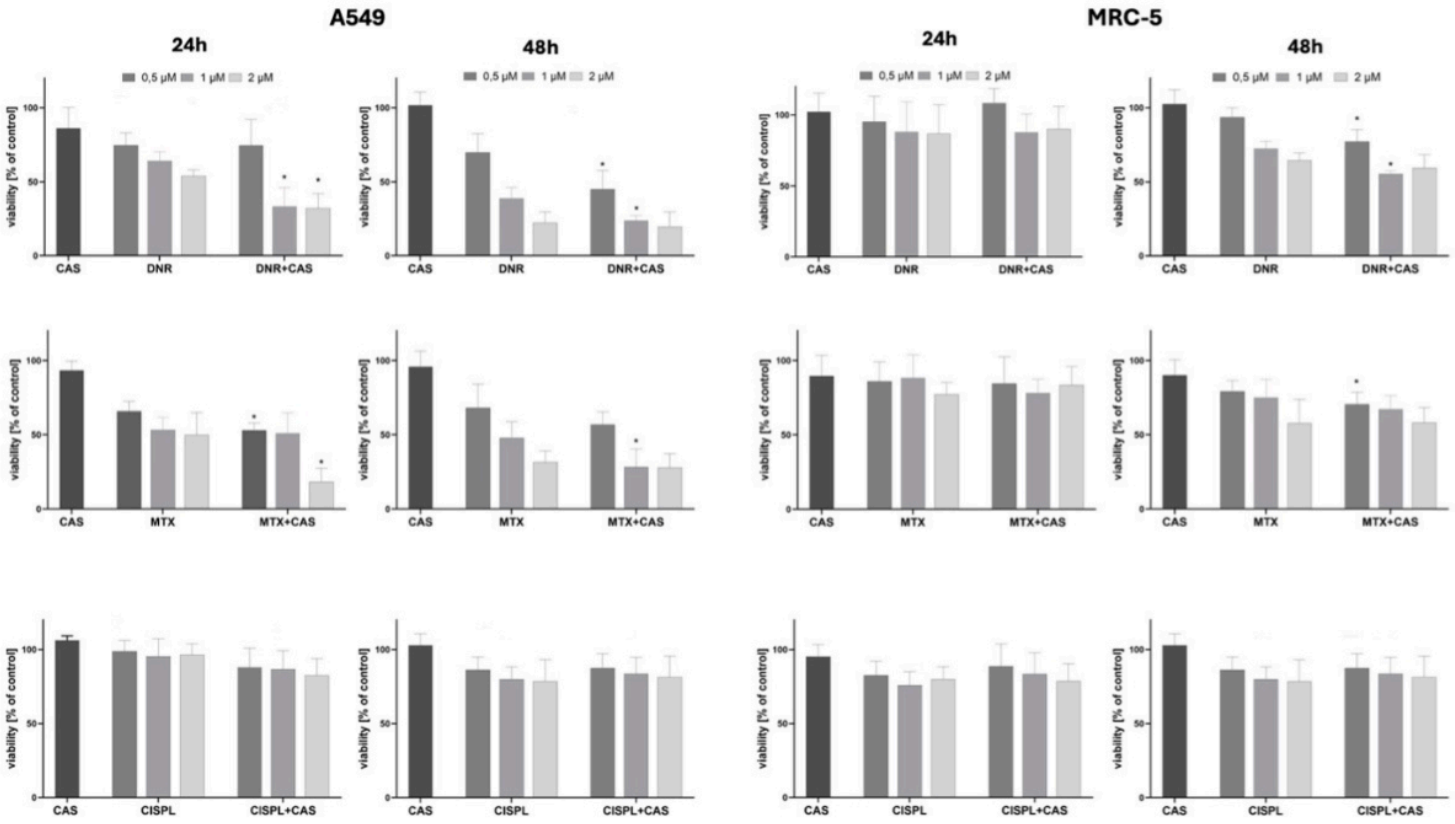


**Figure 1**

**Casticin enhances the chemotherapeutic effects of DNR and MTX in A549 cells (A) with limited cytotoxicity toward non-malignant lung fibroblasts (MRC-5) (B).**Cell viability was analyzed in A549 (A) and MRC-5 cells (B) after 24 h and 48 h of incubation with CAS, DNR, MTX, or CISPL, administered alone or in co-treatment with CAS in concentration of 0,5, 1, and 2 µM. Cell viability is expressed as the percentage of viable cells relative to the control (cells without tested compounds). Data are presented as mean ± SD from three independent experiments. Statistical significance (*) was determined using the Mann–Whitney U test ($p < 0.05$), DNR *vs*. DNR+CAS, MTX *vs*. MTX+CAS or CISPL *vs*. CISPL+CAS.

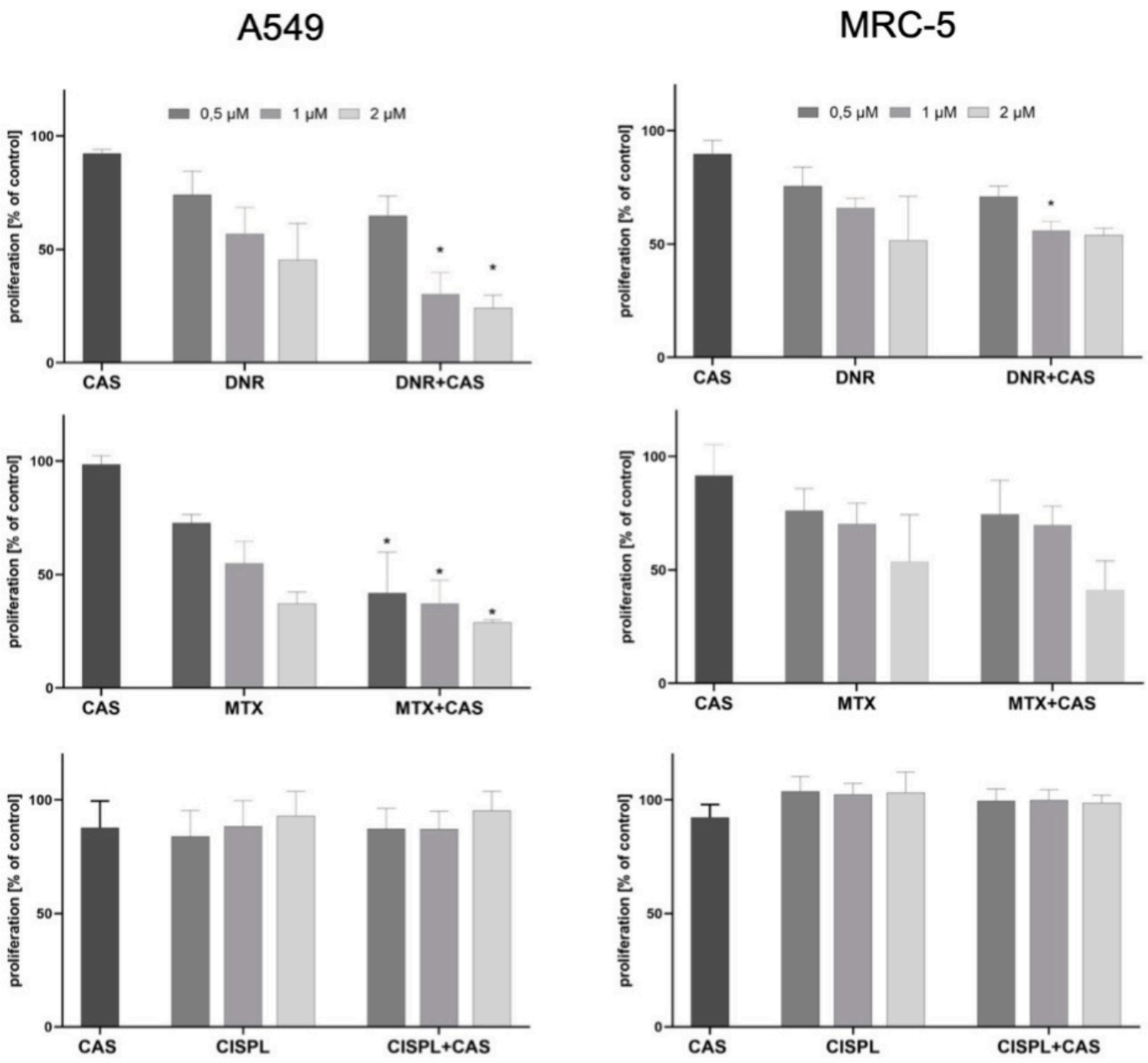


## Figure 2

**Co-treatment with CAS and DNR, MTX inhibit proliferation of A549 cells (A) while no comparable effect was observed in non-malignant MRC-5 fibroblasts (B)**. Cell proliferations was analyzed in A549 (A) and MRC-5 cells (B) after 24 h of incubation with CAS, DNR, MTX, or CISPL, administered alone or in co-treatment with CAS in concentration of 0.5, 1, and 2 µM. Graphs show the mean number of proliferating cells expressed as a percentage of the control (cells without tested compounds) ± SD. Data represent results from three independent experiments. Statistical significance (*) was determined using the Mann–Whitney U test ($p < 0.05$), comparing DNR *vs*. DNR+CAS, MTX *vs*. MTX+CAS or CISPL *vs*. CISPL+CAS.

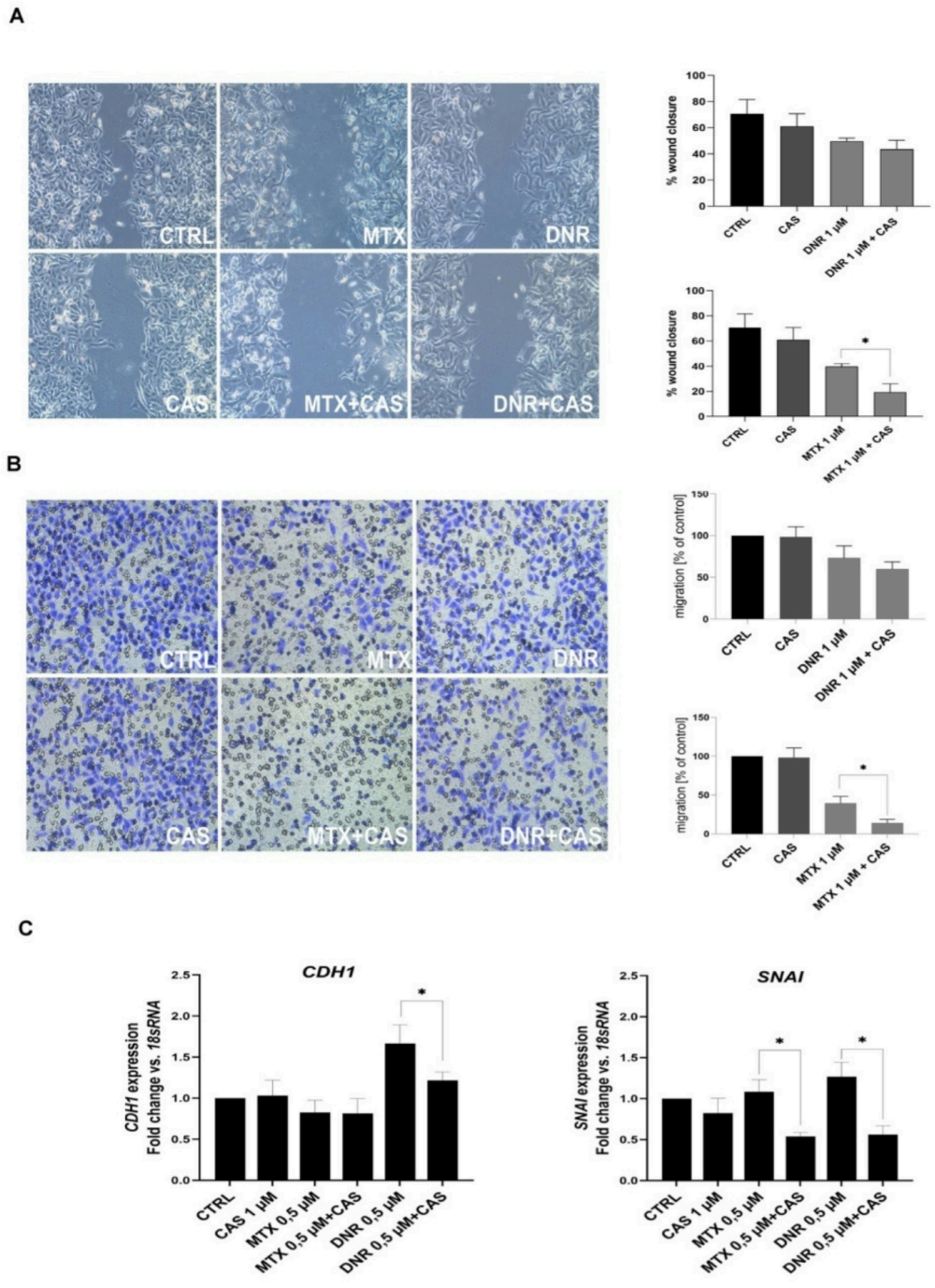


## Figure 5

**Effect of co-treatment with CAS and DNR or MTX on decreasing cell migration assessed by the wound healing assay (A) and Transwell® model (B) and *CDH1* and *SNAI* gene expression (C).** Wound healing assay (A) was performed after 48 h of incubation with DNR or MTX (1 µM) alone or in co-treatment with CAS. Migration through a porous membrane in the Transwell® system (**B**) was evaluated after 24 h of incubation with DNR or MTX (0.5 µM) alone, or in co-treatment with CAS. Gene expression levels of *SNAI*

and *CDH1* (**C**) were analyzed by qPCR after 24 h of treatment. Data are presented as mean ± SD from three independent experiments. Statistical significance (*) was determined using the Mann–Whitney U test ($p < 0.05$), comparing DNR vs. DNR+CAS or MTX vs. MTX+CAS.